Research Article

Received: 25 June 2012 Revised: 1 October 2012 Accepted: 8 October 2012 Published online in Wiley Online Library: 21 December 2012

(wileyonlinelibrary.com) DOI 10.1002/pi.4439

Probing the temperature sensitivity of induction time in latent cure epoxy resins

Amy M Yousefi[a] and Brian J Love[b,c,d]*

Abstract

Two dynamic viscosity datasets for epoxy resins cured at temperatures between 100 and 150 °C were re-analyzed to compare the interpretation of gel times and activation energies using two mathematical models.

Keywords: epoxy resin; cure; viscosity; mathematical modeling; Arrhenius

INTRODUCTION

Efforts to tie dynamic viscosity data associated with polymerization have led to an array of molecular, kinetic and purely empirical models used to predict flow in a range of reactive systems including epoxy resins, acrylates and proteins. These viscosity correlations are important in adhesives and coatings, resin transfer molding and composite resin infiltration, where mold filling and void formation are optimized.[1] Correlating viscosity and other measures with increasing conversion is also of fundamental importance.[2–5] The evolving network structure is a key feature in regulating continued flow. There is interest in defining the structure of the gel point in terms of both physical structure and rate of viscosity advancement.[6,7]

Separately, there have been several different viscosity advancement models for both reactive thermosets and other polymerizing resins.[7–10] Those systems advancing in viscosity and conversion can be characterized based on *n*th-order kinetics where small-molecule behavior is governed by one exponent and larger structures by larger ones identified at higher conversion.[11–17] The gel point is fundamentally linked with a critical extent of reaction at which the formation of macromolecular clusters extends across the sample dimension.[18] It is also correlated with inflection points in the log $\eta(t)$ curve[16] or the maximum rate of viscosity increase.[1] There are other interpretations of the gel point using other analyses including the crossover point between G' and G'',[19,20] the inflection point of G'',[21] or the point where the loss tangent is frequency invariant[22–25] using dynamic mechanical spectroscopy or rheology.

Other nonlinear rheological models have been advanced based on parameters indicative of resin reactivity,[26,27] thermodynamic models similar to the WLF model[8] and other semi-empirical models to describe time-dependent viscosity including our work on the log-Boltzmann sigmoidal model shown in Eqn (1):[8,17,28–30]

$$\log \eta\,(t) = \log \eta_\infty + \frac{\log\,(\eta_0) - \log\,(\eta_\infty)}{1 + e^{(t-t_0)/\Delta t}} \qquad (1)$$

In this equation, η_0 corresponds to the initial viscosity of the formulated resin, η_∞ is linked with the viscosity approaching the torque limit in the rheometer as network formation evolves and t_0 is an induction time, corresponding to the 50% traversal between $\log \eta_0$ and $\log \eta_\infty$, and most closely associates with the gel time. The value $4 \times \Delta t$ corresponds to the period associated with the sigmoidal transition region as viscosity changes from the initial condition to the final gel condition. Thus, it is these two time constants that define how long the induction period is before gel formation and how fast one toggles between the initial and terminal viscosities.

Among the most predominant phenomenological models to represent dynamic viscosity is the first-order isothermal model:[31]

$$\log \eta\,(t) = \log \eta_0 + kt \qquad (2)$$

where $\eta(t)$ is the time-dependent viscosity, η_0 is some starting viscosity at which crosslinking occurs, k is related to the rapidity of the viscosity increase and t is the time. Equation (2) can be extended by assuming an Arrhenius temperature dependence for η_0 and k as follows:[32]

$$\ln \eta\,(t) = \ln \eta_0 + \frac{\Delta E_\eta}{RT} + tk_0 \exp\left(\frac{\Delta E_k}{RT}\right) \qquad (3)$$

In this equation, T is the temperature, η_0 is the reference viscosity, ΔE_η is the Arrhenius activation energy for viscosity, R is the universal gas constant, k_0 is the kinetic analogue of η_0 and ΔE_k is the kinetic analogue of ΔE_η. All the presented models

* *Correspondence to: Brian J Love, Department of Materials Science and Engineering, University of Michigan, Ann Arbor, MI 48104, USA. E-mail: bjlove@umich.edu*

a *Bioengineering, Chemical and Paper Engineering Department, Miami University, Oxford, OH, 45056, USA*

b *Department of Materials Science and Engineering, University of Michigan, Ann Arbor, MI, 48104, USA*

c *Department of Biomedical Engineering, University of Michigan, Ann Arbor, MI, 48104, USA*

d *Department of Biologic and Materials Sciences (Dentistry), University of Michigan, Ann Arbor, MI, 48104, USA*

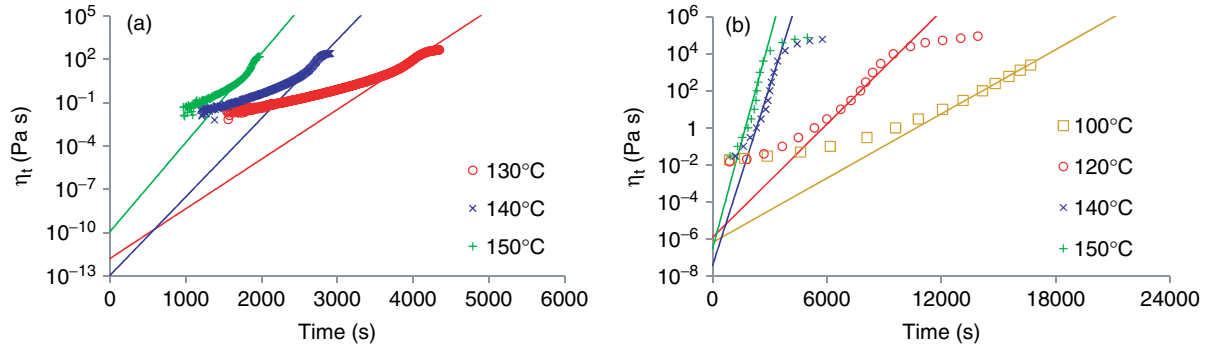

Figure 1. Data from (a) Mounif *et al.*[25] and (b) Naffakh *et al.*[34] analyzed using the first-order model. The inflection in viscosity with time is identified as the gel point.

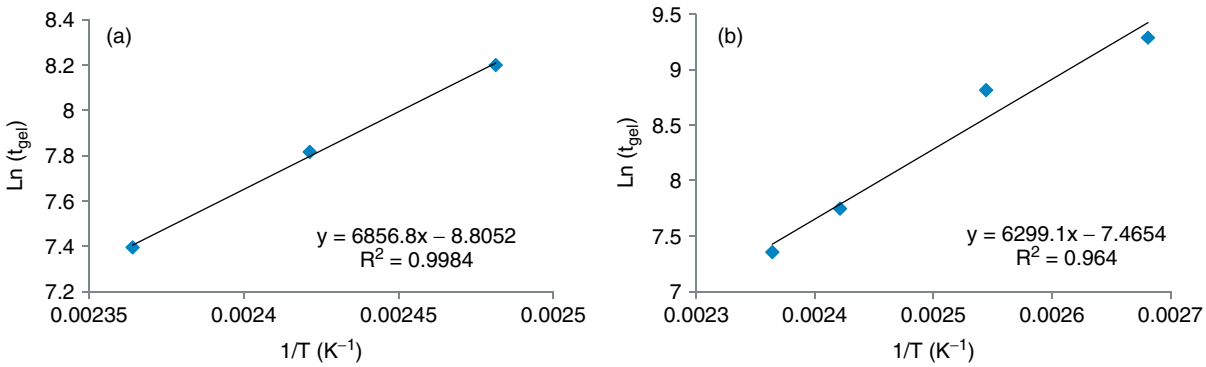

Figure 2. Arrhenius plots representing the gel time as a function of temperature based on the first-order analysis: (a) Mounif *et al.*[25] and (b) Naffakh *et al.*[34]

capture the viscosity increase within a certain range of processing conditions. There are others that have also been developed (see Halley and Mackay[8]), but in this work we chose to probe these models based on both their simplicity and their reported accuracy in representing dynamic viscosity at different cure temperatures. These analyses enabled us to predict the viscosity advancement in order to effectively represent the different stages of functional crosslinking.

It is perceived that with latent cure systems, the deviation in the initial viscosity, η_0, with time is quite small in the pre-gel state. Mounif *et al.* point to a time–temperature equivalence during the initial viscosity advancement stages that may be a predictor of network growth, although their primary focus was very early in conversion with viscosities below 10 Pa s.[25] Depending on the network being formed, there are theoretical determinations of what conversion is necessary to form the gel. We chose to evaluate whether this same dataset had a similar Boltzmann-like sigmoidal behavior and how well the sigmoidal model and first-order models matched up over the wider conversion curve. The sigmoidal chemorheological model has resolved epoxy conversion in filled systems such as for chip underfill.[30,33] Our interest was whether it could also predict dynamic viscosity in more latent cure resin infiltrators such as that used by Mounif *et al.*[25] and Naffakh *et al.*[34] There are some interesting elements to comparing these separate contributions together. They used the same resin and hardener and had some overlapping resin cure conditions. They also both reported dynamic viscosity data which could be extracted by us for a cross-comparison.

In the study reported here we compared both a Boltzmann log-sigmoidal model fixing the initial viscosity and a first-order isothermal model for viscosity advancement where the inflection in slopes is identified as the gel point. The Boltzmann analysis yields three parameters, two time constants associated with the shape of the curve and a plateau viscosity associated with either the torque limit of the rheometer or the hindered motion of the resin in the glassy state. The first-order model yielded slopes in both the resin and gel states and a separate gel time. Interpretations of the Boltzmann and first-order models allow alternative determinations of the gel times that yield similar activation energies to those identified in the original analyses. Pragmatically, creation of dynamic viscosity models allows their incorporation into predictive flow models based on other extensive property changes with temperature and pressure.

EXPERIMENTAL

The original experiments re-analyzed here used diglycidyl ether of bisphenol A (DGEBA), with an epoxy equivalent weight of 178 g mol^{-1}, mixed with diethyltoluenediamine, with an amine equivalent weight of 45 g mol^{-1}. For both protocols, the hardener was added to DGEBA in a stoichiometric ratio and mixed. Mounif *et al.* mention their formulations were mixed at 55 °C in an oil bath and degassed under vacuum for 20 min at 40 °C.[25] Again for both protocols, they were then cured while simultaneously tracking conversion using rheometry, Mounif *et al.*[25] using a range of cure temperatures between 120 and 150 °C while Naffakh *et al.*[34] used 100–150 °C.

Rheological properties were originally measured by Mounif *et al.* with an ARES rheometer (TA Instruments) in parallel plate mode while Naffakh *et al.* used an RDAII. There are probably some minor differences in detail as to how these experiments were executed but essentially the resins were conveyed to the plate surfaces and a

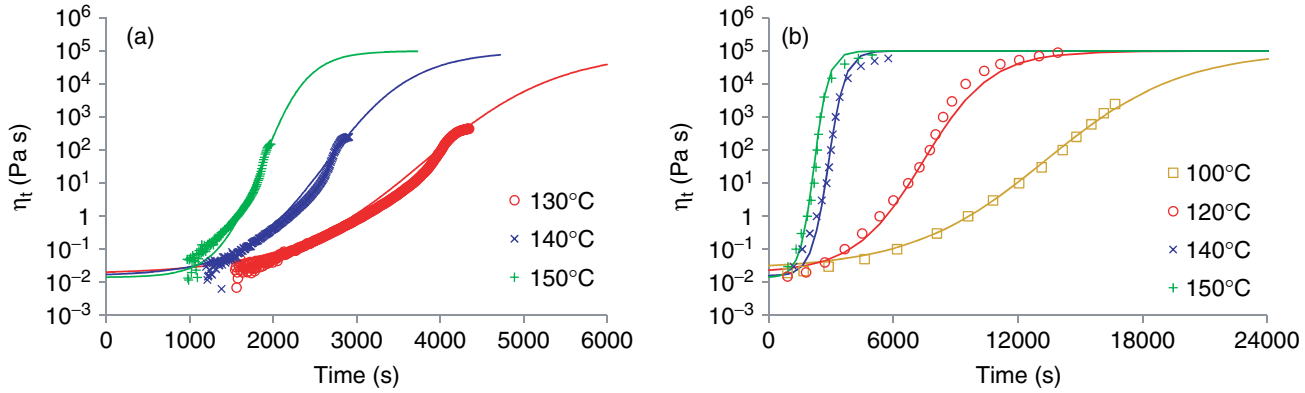

Figure 3. Sigmoidal determination including the raw data from (a) Mounif *et al.*[25] and (b) Naffakh *et al.*,[34] and the corresponding fits with fixed initial and final viscosity of the gel of 1×10^5 Pa s.

Table 1. Gel time determinations (Mounif *et al.*[25] dataset)

	Gel time (s)			
Temperature (°C)	Mounif *et al.*	Sigmoidal model (constant η_∞)	Sigmoidal model, (variable η_∞)	First-order model
130	3780	2190	2190	3640
140	2520	1600	1830	2480
150	1740	1320	1190	1630

time sweep was started for each isothermal experiment. They both used a time ramp at a multi-frequency mode to determine the gel time considering the independence of the loss factor on frequency as a criterion of gel point. Dynamic DSC experiments were also performed to determine the glass transition temperature, T_g, before and after crosslinking. T_g was interpreted by Mounif *et al.* as the inflection point of the second-order endothermic transition.[25]

RESULTS

We obtained the datasets from Mounif *et al.* that were imported into Origin8 (OriginLab, Northampton, MA), a mathematical analysis package equipped with a series of curve analysis subroutines. We extracted the Naffakh *et al.* work independently. While Mounif *et al.* focused on the initial changes in viscosity, we used the entire datasets for both studies to resolve whether other models might represent a wider time spectrum of $\eta(t)$. Strain sweeps performed at each temperature were compared as a function of time to yield a time-dependent viscosity at each temperature isotherm.

First-order isothermal model analysis

The data were fitted using a first-order-type model as shown in Eqn (2). Conceptually, when the data are plotted in the form of log $\eta(t)$ *versus* t as shown in Fig. 1, it seems evident that above 10 Pa s there is a slope inflection corresponding to the increase in fluid resistance with continued thermoset advancement. This inflection occurs at all temperatures. Although the discrepancy between the experimental data and the fits at lower viscosities is negligible, given the logarithmic scale of these graphs, it is clear that the first-order model is not able to capture the viscosity plateau at the end of the cure reactions.

Using the first-order isothermal model, the exponent associated with the rapid rise in resin viscosity increases from 0.21 to 0.37 min^{-1} when the cure temperature increases from 130 to 150 °C (Mounif *et al.* dataset). This is comparable to slopes determined from Karkanas *et al.* using the same resin with a different array of amine hardeners but curing in the same temperature regime.[35] The corresponding exponent for the Naffakh *et al.* dataset ranges between 0.03 and 0.23 min^{-1} when the cure temperature is raised from 100 to 150 °C. The time associated with slope inflection was also extracted to identify the gel time. An Arrhenius determination relating the gel time as a function of $1/T$ shown in Fig. 2 resolves an activation energy to trigger gelation of 57 kJ mol^{-1} (Mounif *et al.*) and 52 kJ mol^{-1} (Naffakh *et al.*) based on the first-order isothermal model analysis.

Sigmoidal analysis

We also used the sigmoidal analysis function to fit these datasets, as shown in Eqn (1). The analysis allowed for any one parameter to be fixed while optimizing the other variables. Given that another dataset using DGEBA resin shows a lower initial viscosity of 0.01 Pa s at 155 °C,[36] we fixed the initial viscosity at each temperature, weakly depending on temperature based on an Arrhenius activation energy for flow. Final gel viscosities in the plateau region were also fixed at 1×10^5 Pa s based on the work by Naffakh *et al.*[34] for the same resin. Example analyses fixing η_0 are shown in Fig. 3 for sigmoidal analyses at 130, 140 and 150 °C reported by Mounif *et al.*[25] as well as at 100, 120, 140 and 150 °C reported by Naffakh *et al.*[34]

It is apparent that the sigmoidal model effectively represents the temperature-dependent dynamic viscosity response of the advancing resin. It is also evident that the interval of viscosity increase is shorter at elevated temperature. The dynamic viscosity

Table 2. Model parameters extracted from the various analyses (Mounif *et al.*[25] dataset)

Temperature (°C)	Sigmoidal model (constant η_∞)	Sigmoidal model (variable η_∞)	First-order model
130	$\eta_\infty = 1 \times 10^5$ Pa s $\eta_0 = 1.78 \times 10^{-2}$ Pa s $t_0 = 3800$ s $\Delta t = 804$ s	$\eta_\infty = 1 \times 10^5$ Pa s $\eta_0 = 1.78 \times 10^{-2}$ Pa s $t_0 = 3800$ s $\Delta t = 804$ s	$\eta_0 = 1.67 \times 10^{-12}$ Pa s $k = 0.21$ min^{-1}
140	$\eta_\infty = 1 \times 10^5$ Pa s $\eta_0 = 1.58 \times 10^{-2}$ Pa s $t_0 = 2630$ s $\Delta t = 515$ s	$\eta_\infty = 7.94 \times 10^4$ Pa s $\eta_0 = 1.58 \times 10^{-2}$ Pa s $t_0 = 2680$ s $\Delta t = 427$ s	$\eta_0 = 1.13 \times 10^{-13}$ Pa s $k = 0.33$ min^{-1}
150	$\eta_\infty = 1 \times 10^5$ Pa s $\eta_0 = 1.41 \times 10^{-2}$ Pa s $t_0 = 1870$ s $\Delta t = 273$ s	$\eta_\infty = 6.31 \times 10^4$ Pa s $\eta_0 = 1.41 \times 10^{-2}$ Pa s $t_0 = 1800$ s $\Delta t = 306$ s	$\eta_0 = 1.19 \times 10^{-10}$ Pa s $k = 0.37$ min^{-1}

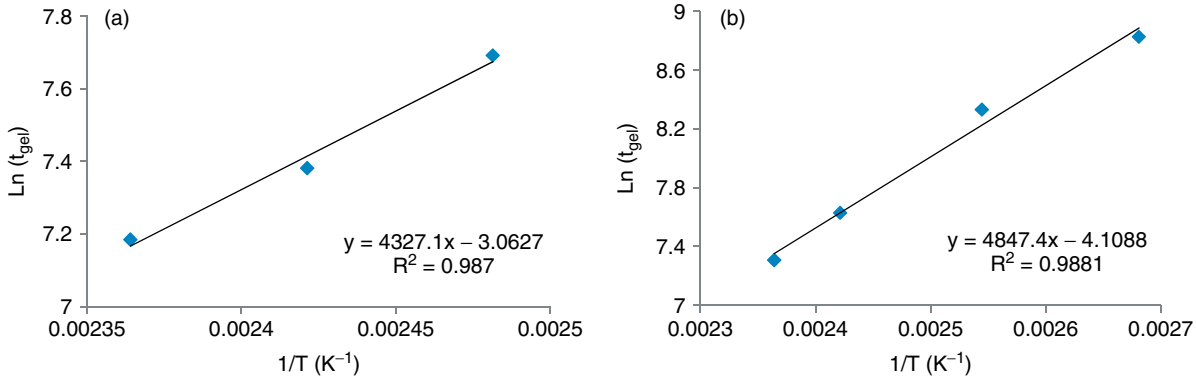

Figure 4. Arrhenius plots based on the sigmoidal model using a fixed plateau viscosity of 1×10^5 Pa s: (a) Mounif *et al.*[25] and (b) Naffakh *et al.*[34]

Table 3. Gel time determinations (Naffakh *et al.*[34] dataset)

Temperature (°C)	Gel time (s)		
	Sigmoidal model (constant η_∞)	Sigmoidal model (variable η_∞)	First-order model
100	6 820	3 310	10 800
120	4 150	1 660	6 720
140	2 050	390	2 310
150	1 490	321	1 560

is much broader between 100 and 130 °C as opposed to 150 °C. The numerical extractions from both analyses are given in Tables 1–4.

An objective determination of a gel time can be resolved by taking the slope of the dynamic viscosity curve and identifying the time at which this intersects the initial viscosity. This occurs at a time on the sigmoidal curve associated with the midpoint of the log $\eta(t)$ curve less two times the quantity Δt. The Arrhenius dependence of gel time based on the sigmoidal model is shown in Fig. 4, identifying an activation energy of 36 kJ mol^{-1} (Mounif *et al.*) and 40 kJ mol^{-1} (Naffakh *et al.*).

Alternatively, fixing η_0 and allowing a variable η_∞ leads to minor differences in t_0 and Δt with a better fit shown in Fig. 5 for sigmoidal analyses at the four temperatures reported by Naffakh *et al.*[34] The corresponding Arrhenius dependence of gel time (Fig. 6) results in a determination of an activation energy of 43 kJ mol^{-1} (Mounif *et al.*) and 40 kJ mol^{-1} (Naffakh *et al.*).

DISCUSSION

The interpretation of a gel time extracted using the first-order and sigmoidal models reinforces the original analysis by Mounif *et al.* who resolved the invariance in $\tan\delta$ as a function of frequency during isothermal curing. Based on the re-analysis of the Mounif *et al.*[25] data, we determine an activation energy for gelation of 57 kJ mol^{-1} using the first-order model, only slightly smaller than the 60 kJ mol^{-1} resolved by Mounif *et al.* Naffakh *et al.*[34] using a larger cure temperature range found an activation energy of 55 kJ mol^{-1}. We determine an activation energy of 52 kJ mol^{-1} for the data published by Naffakh *et al.* There are countless studies to evaluate the relative activation energy for a combination of resins + aromatic amine hardeners, typically in the range 50–70 kJ mol^{-1} based on comments by Ishii and Ryan.[37] Perhaps focusing on the initial stages of the viscosity increase and a lower cure temperature biases the interpretation of activation energy to discount the autocatalytic contribution from the exothermic epoxide reaction leading to a larger perceived barrier for advancement.

The sigmoidal analysis emphasizes the distinctions in the early phases of conversion, and leads to a more diverse advancement profile depending on isothermal cure temperature. When extracted from the initial viscosity regime of the resin, we resolve a lower activation energy of between 36 and 43 kJ mol^{-1}. We observe the expected decrease in Δt with increasing isothermal conversion. Scott and Saad reported on the activation energy of DGEBA from DSC and dielectric measurements and resolved activation energies as low as 37 kJ mol^{-1}.[38] Clearly the increase in

Table 4. Model parameters extracted from the various analyses (Naffakh *et al.*[34] dataset)

Temperature (°C)	Sigmoidal model (constant η_∞)	Sigmoidal model (variable η_∞)	First-order model
100	$\eta_\infty = 1 \times 10^5$ Pa s $\eta_0 = 2.51 \times 10^{-2}$ Pa s $t_0 = 13\,300$ s $\Delta t = 3260$ s	$\eta_\infty = 2 \times 10^5$ Pa s $\eta_0 = 2.51 \times 10^{-2}$ Pa s $t_0 = 13\,600$ s $\Delta t = 3310$ s	$\eta_0 = 6.57 \times 10^{-7}$ Pa s $k = 0.03$ min^{-1}
120	$\eta_\infty = 1 \times 10^5$ Pa s $\eta_0 = 2.00 \times 10^{-2}$ Pa s $t_0 = 7420$ s $\Delta t = 1630$ s	$\eta_\infty = 1.26 \times 10^5$ Pa s $\eta_0 = 2.00 \times 10^{-2}$ Pa s $t_0 = 7470$ s $\Delta t = 1660$ s	$\eta_0 = 1.24 \times 10^{-6}$ Pa s $k = 0.06$ min^{-1}
140	$\eta_\infty = 1 \times 10^5$ Pa s $\eta_0 = 1.58 \times 10^{-2}$ Pa s $t_0 = 2870$ s $\Delta t = 407$ s	$\eta_\infty = 7.94 \times 10^4$ Pa s $\eta_0 = 1.58 \times 10^{-2}$ Pa s $t_0 = 2860$ s $\Delta t = 390$ s	$\eta_0 = 3.72 \times 10^{-8}$ Pa s $k = 0.19$ min^{-1}
150	$\eta_\infty = 1 \times 10^5$ Pa s $\eta_0 = 1.41 \times 10^{-2}$ Pa s $t_0 = 2190$ s $\Delta t = 351$ s	$\eta_\infty = 6.31 \times 10^4$ Pa s $\eta_0 = 1.41 \times 10^{-2}$ Pa s $t_0 = 2180$ s $\Delta t = 321$ s	$\eta_0 = 3.09 \times 10^{-7}$ Pa s $k = 0.23$ min^{-1}

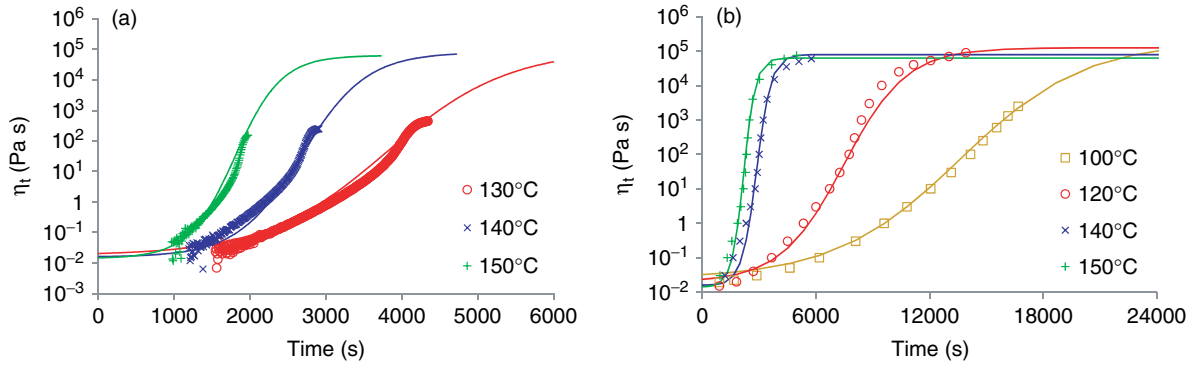

Figure 5. Sigmoidal viscosity *versus* time curves showing the effect of liberating the plateau viscosity for each isothermal advancement curve: (a) Mounif *et al.*[25] and (b) Naffakh *et al.*[34]

Brownian motion at elevated temperature increases the number of hardener–resin interactions and increases the rate of conversion with the number of encounters.

These re-analyses are subject to the constraint of rheometer accuracy in this low-viscosity regime. The sigmoidal model has an added constraint requiring some sort of determination of an upper limit for viscosity to be included. There are published studies of resin mixtures reporting initial viscosities in the region of 1×10^{-3} Pa s. Applying fixed constraints based on the physical significance of the initial and gel viscosity leads to a larger physical significance of the time constants associated with gel formation and dynamic changes in the network structure.

CONCLUSIONS

Previously published dynamic rheology data have been re-analyzed using both the first-order isothermal and sigmoidal models. Refinements of the sigmoidal four-parameter model to fix both the initial viscosity condition and the upper limit for the gel viscosity yielded two time constants while the first-order model yielded both a gel time and a conversion ratio.

The first-order model interpretation of the viscosity advancement data shows a clear slope change leading to an unambiguous interpretation of the gel time. We interpret a lower activation energy for gelation of 52–57 kJ mol^{-1} when considering the full datasets of Mounif *et al.* and Naffakh *et al.*, smaller than that identified by Mounif *et al.*, and more representative of that of Naffakh *et al.* using the same resin system.

The sigmoidal model also yielded an objective determination of a time when the viscosity deviates from the initial viscosity condition. Based on this analysis, we determine an activation energy of between 36 and 43 kJ mol^{-1} depending on whether the plateau viscosity is a fixed parameter or a floating variable as a function of temperature. Supporting evidence for these lower activation energies of cure advancement is included.

Both analyses effectively represent the data and allow for the construction of relevant kinetic models of viscosity advancement with time constants that can help represent the latency and the corresponding periods of functional crosslinking.

ACKNOWLEDGEMENTS

The authors acknowledge Eskandar Mounif and Veronique Bellenger for graciously providing us access to the original datasets, Miami University for Amy Yousefi's sabbatical, and Caroline Dove and Thibaut Savart for completing some of the initial data analysis.

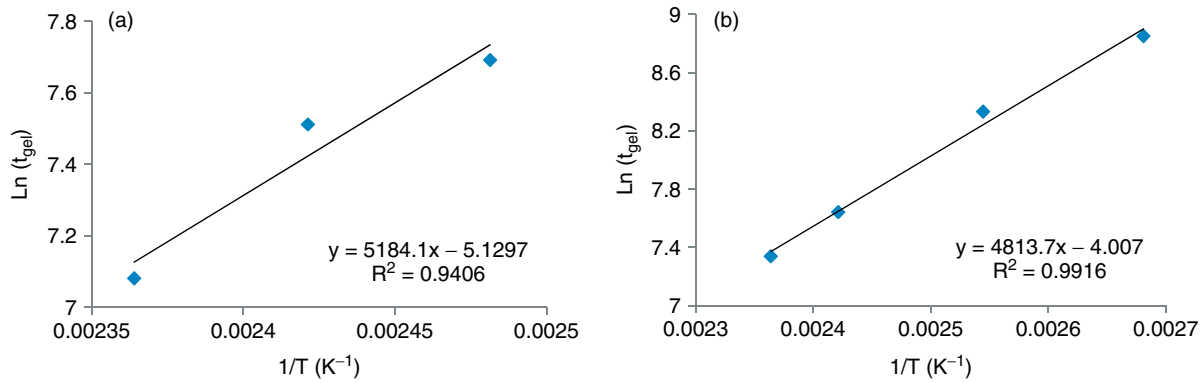

Figure 6. Arrhenius plots based on the sigmoidal model using a variable plateau viscosity: (a) Mounif *et al*.[25] and (b) Naffakh *et al*.[34]

REFERENCES

1 Ivankovic M, Incarnato L, Kenny JM and Nicolais L, *J Appl Polym Sci* **90**:3012–3019 (2003).
2 Kamal MR, *Polym Eng Sci* **14**:231–239 (1974).
3 Kamal M and Sourour S, *Polym Eng Sci* **13**:59–64 (1973).
4 Lipshitz SD and Macosko CW, *J Appl Polym Sci* **21**:2029–2039 (1977).
5 Lipshitz SD and Macosko CW, *Polym Eng Sci* **16**:803–810 (1976).
6 Achilias DS, *Macromol Theory Simul* **16**:319–347 (2007).
7 Achilias DS and Kiparissides C, *Macromolecules* **25**:3739–3750 (1992).
8 Halley PJ and Mackay ME, *Polym Eng Sci* **36**:593–609 (1996).
9 Achilias DS and Sideridou ID, *Macromolecules* **37**:4254–4265 (2004).
10 Yousefi A, Lafleur PG and Gaurvin R, *Polym Compos* **18**:157–168 (1997).
11 Sun YY, Zhang ZQ and Wong CP, *IEEE Trans Components Packag Technol* **29**:190–197 (2006).
12 Sun YY, Zhang ZQ and Wong CP, *Macromol Mater Eng* **290**:1204–1212 (2005).
13 Cioffi M, Ganzeveld KJ, Hoffmann AC and Janssen L, *Polym Eng Sci* **44**:179–185 (2004).
14 Cioffi M, Ganzeveld KJ, Hoffmann AC and Janssen L, *Polym Eng Sci* **42**:2383–2392 (2002).
15 Cioffi M, Hoffmann AC and Janssen L, *Polym Eng Sci* **41**:595–602 (2001).
16 Love BJ and Piguet-Ruinet F, *J Appl Polym Sci* **106**:3605–3609 (2007).
17 Love BJ, Piguet-Ruinet F and Teyssandier F, *J Polym Sci B: Polym Phys* **46**:2319–2325 (2008).
18 Chambon F and Winter HH, *J Rheol* **31**:683–697 (1987).
19 Haddadi H, Famili MHN, Nazokdast E and Moradi S, *Iranian Polym J* **15**:967–977 (2006).
20 Tung CYM and Dynes PJ, *J Appl Polym Sci* **27**:569–574 (1982).
21 Apicella A, Nicolais L, Iannone M and Passerini P, *J Appl Polym Sci* **29**:2083–2096 (1984).
22 Boey FYC and Qiang W, *J Appl Polym Sci* **76**:1248–1256 (2000).
23 Winter HH, *Polym Eng Sci* **27**:1698–1702 (1987).
24 Matejka L, *Polym Bull* **26**:109–116 (1991).
25 Mounif E, Bellenger V and Tcharkhtchi A, *J Appl Polym Sci* **108**:2908–2916 (2008).
26 Yang YS and Suspene L, *Polym Eng Sci* **31**:321–332 (1991).
27 Malkin AY, Kulichikhin SG, Kerber ML, Gorbunova IY and Murashova EA, *Polym Eng Sci* **37**:1322–1330 (1997).
28 Teyssandier F and Love BJ, *J Appl Polym Sci* **120**:1367–1371 (2011).
29 Love BJ, Teyssandier F, Sun YY and Wong CP, *Macromol Mater Eng* **293**:832–835 (2008).
30 Teyssandier F, Sun YY, Wong CP and Love BJ, *Macromol Mater Eng* **293**:828–831 (2008).
31 White RP, *Polym Eng Sci* **14**:50–57 (1974).
32 Roller MB, *Polym Eng Sci* **26**:432–440 (1986).
33 Teyssandier F, Ivankovic M and Love BJ, *J Appl Polym Sci* **115**:1671–1674 (2010).
34 Naffakh M, Dumon M and Gerard J-F, *J Appl Polym Sci* **102**:4228–4237 (2006).
35 Karkanas PI and Partridge IK, *J Appl Polym Sci* **77**:2178–2188 (2000).
36 Simpson JO and Bidstrup-Allen SA, *J Polym Sci B: Polym Phys* **33**:55–62 (1995).
37 Ishii Y and Ryan ME, *Macromolecules* **33**:167–176 (2000).
38 Scott EP and Saad Z, *Polym Eng Sci* **33**:1165–1169 (1993).

